



Binary black hole mergers from hierarchical triples in open clusters

Dylan Britt,^{1,2} Ben Johanson,¹ Logan Wood,^{1,3} M. Coleman Miller^{1,4} and Erez Michaely¹  

¹Department of Astronomy, University of Maryland, College Park, MD 20742, USA

²Kavli Institute for Particle Astrophysics & Cosmology, Stanford University, PO Box 2450, Stanford, CA 94305, USA

³Department of Physics and Astronomy, George Mason University, Fairfax, VA 22030, USA

⁴Joint Space-Science Institute, University of Maryland, College Park, MD 20742, USA

Accepted 2021 May 26. Received 2021 May 11; in original form 2021 March 26

ABSTRACT

A promising channel for producing binary black hole mergers is the Lidov–Kozai orbital resonance in hierarchical triple systems. While this mechanism has been studied in isolation, the distribution of such mergers in time and across star-forming environments is not well characterized. In this work, we explore Lidov–Kozai-induced black hole mergers in open clusters, combining semi-analytical and Monte Carlo methods to calculate merger rates and delay times for nine different population models. We predict a merger rate density of $\sim 1\text{--}10 \text{ Gpc}^{-3} \text{ yr}^{-1}$ for the Lidov–Kozai channel in the local Universe, and all models yield delay-time distributions in which a significant fraction of binary black hole mergers (e.g. $\sim 20\text{--}50$ per cent in our baseline model) occur during the open cluster phase. Our findings suggest that a substantial fraction of mergers from hierarchical triples occur within star-forming regions in spiral galaxies.

Key words: celestial mechanics – galaxies: clusters: general.

1 INTRODUCTION

The detection of binary black hole (BBH) mergers via gravitational wave (GW) emission became routine by the O3 observational run of the LIGO and Virgo collaborations. To date, tens of BBH mergers have been detected, with an overall merger rate density of $\mathcal{R}_{\text{BBH}} = 23.9^{+14.9}_{-8.6} \text{ Gpc}^{-3} \text{ yr}^{-1}$ (Abbott et al. 2020). The identification of relevant channels that lead to mergers via GW emission is an ongoing endeavour that spans a number of subfields, including orbital dynamics, stellar evolution, and dynamics on the scale of galaxies.

Channels for BBH mergers may be grouped into four broad categories. The first, isolated binary stellar evolution of massive stars (e.g. Tutukov & Yungelson 1973, 1993; Lipunov, Postnov & Prokhorov 1997; Bethe & Brown 1998; Portegies Zwart & Yungelson 1998; Kalogera 2000; Voss & Tauris 2003; Kalogera et al. 2007; Belczynski et al. 2008, 2016; Mandel & O’Shaughnessy 2010; Dominik et al. 2012, 2013, 2015; de Mink & Belczynski 2015; Eldridge et al. 2017; Giacobbo, Mapelli & Spera 2018; Olejak et al. 2020), proposes that some massive stellar binaries evolve to short-period binaries prior to either star forming a black hole (BH). One type of such evolution occurs during one or two common envelope episodes, in which one star swells during the giant phase, imparting drag on the other and shrinking their mutual orbit. The total orbital energy loss is directly related to the amount of energy transferred to the envelope of the giant star. If the energy transfer is too efficient, then the binary merges before the objects turn into BHs; if the transfer is too inefficient, then the binary does not lose enough orbital energy to merge via GW emission. The result is a short-period stellar binary that then evolves to a BBH and merges via GW emission within a

Hubble time. Studies of this channel predict a delay-time distribution (DTD) $\propto t^{-1}$ that starts 10–100 Myr after star formation. They also predict no measurable eccentricity in the LIGO detection band (due to circularization during the binary interaction phase and the subsequent circularization from gravitational radiation) and merger rate densities of $\sim 10^{-2}$ to $10^3 \text{ Gpc}^{-3} \text{ yr}^{-1}$.

Another isolated binary formation scenario is the chemically homogeneous stellar evolution (de Mink & Mandel 2016; Mandel & de Mink 2016; Marchant et al. 2016). In this scenario, a massive binary that is close to contact experiences intense internal mixing that keeps the stars chemically homogeneous while the cores are burning hydrogen. The hydrogen in the star is thus nearly exhausted and thus a common envelope phase is avoided. The predicted BBH merger rate is up to $500 \text{ Gpc}^{-3} \text{ yr}^{-1}$ (de Mink & Mandel 2016).

A second merger channel is dynamical in nature and proposes that existing BBHs are induced to merge in dense environments such as galactic centres, active galactic nucleus accretion discs, or globular clusters. In these settings, BBHs experience strong gravitational interactions with individual stars or high-multiplicity systems, and these interactions tend to harden the target binaries and may increase their eccentricities (Kulkarni, Hut & McMillan 1993; Sigurdsson & Phinney 1993; Portegies Zwart & McMillan 2000; Madau & Rees 2001; Miller & Hamilton 2002a; Gültekin, Miller & Hamilton 2004, 2006; Miller & Lauburg 2009; McKernan et al. 2012; Samsing, MacLeod & Ramirez-Ruiz 2014; Rodriguez, Chatterjee & Rasio 2016; Stone, Metzger & Haiman 2017; Banerjee 2018; Fragione & Kocsis 2018; Hamers et al. 2018; Leigh et al. 2018; Rodriguez et al. 2018, 2021). Models of these interactions predict merger rate densities of $\sim 2\text{--}25 \text{ Gpc}^{-3} \text{ yr}^{-1}$.

The third channel concerns mergers of initially wide, isolated systems, either binaries or triples, in the field of the host galaxy (Michaely & Perets 2019, 2020; Michaely 2021). For wide systems,

* E-mail: erezmichaely@gmail.com

the field of the host galaxy is considered a collisional environment due to frequent flyby interactions with field stars. These interactions are capable of exciting the eccentricity (in the case of binaries) or outer eccentricity (in case of triples), with the result that mergers occur via increased GW emission (binaries) or three-body instabilities (triples). Predicted BBH merger rate densities for this channel are $\sim 1\text{--}100 \text{ Gpc}^{-3} \text{ yr}^{-1}$.

The fourth merger channel, and the focus of this paper, is secular evolution in hierarchical triple systems. These systems reside either in the field of the host galaxy (e.g. Antonini et al. 2016; Antonini, Toonen & Hamers 2017; Silsbee & Tremaine 2017; Liu & Lai 2018; Vigna-Gómez et al. 2021) or in dense environments (Miller & Hamilton 2002b; Antonini, Murray & Mikkola 2014; Kimpson et al. 2016; Samsing & D’Orazio 2018; Hamilton & Rafikov 2019; Martinez et al. 2020). Additionally, there are cases in which the third object is the supermassive BH in the centre of the host galaxy (Antonini & Perets 2012; Petrovich & Antonini 2017; Hoang et al. 2018; Fragione et al. 2019; Wang et al. 2020). In this channel, a BBH experiences secular effects due to its tertiary companion in the form of the Lidov–Kozai resonance (Kozai 1962; Lidov 1962; Harrington 1968; Lidov & Ziglin 1976; Innanen et al. 1997; Ford, Kozinsky & Rasio 2000; Blaes, Lee & Socrates 2002); for a recent review, see Naoz (2016). In this resonance, the eccentricity of the BBH experiences cyclic changes that boost the GW emission rate and lead to a merger. Predicted merger rate densities due to this channel are $\sim 0.5\text{--}15 \text{ Gpc}^{-3} \text{ yr}^{-1}$.

Distinguishing the various channels for producing BBH mergers is important, given that each may yield mergers with particular observational signatures and with different spatial or temporal distributions. BBH mergers in open clusters have been studied previously via N -body simulations (Banerjee 2018; Di Carlo et al. 2019, 2020; Kumamoto, Fujii & Tanikawa 2019; González et al. 2021; Weatherford et al. 2021), which predict merger rate densities of $\sim 0.3 \text{ Gpc}^{-3} \text{ yr}^{-1}$ in these environments. Michaely & Perets (2018) found that a small fraction, up to fraction of a per cent, of mergers are expected to occur extremely close in time to the formation of the second BH, specifically within years to decades following the supernova. Open clusters are loosely bound groups of young stars with stellar number densities $n_* \sim 0.1\text{--}10 \text{ pc}^{-3}$ and typical velocity dispersions $\sigma \sim 1\text{--}5 \text{ km s}^{-1}$ (Moraux 2016). We assume that effectively all star formation occurs in these clusters (Lada & Lada 2003), which remain bound for lifetimes ranging from $\sim 100 \text{ Myr}$ for the sparsest examples to a few Gyr for the densest clusters (Moraux 2016).

In this work, we apply semi-analytical modelling and Monte Carlo simulations to the hierarchical triple channel, studying a set of models describing different initial triple system populations. For each model, we calculate the total BBH merger rate density as well as the cumulative distribution of mergers as a function of time since star formation; this is known as the DTD. In particular, we calculate the fraction of mergers that occur while a triple still resides in its birth cluster. The main aim of this work is to estimate, out of the total population of mergers induced by secular evolution, which fraction of mergers occur during the open cluster phase.

We begin by describing our semi-analytical treatment of BBH mergers induced by the secular Lidov–Kozai resonance in Section 2. In Section 3, we then establish our numerical approach and the different population models considered. Section 4 presents the simulation results, including the DTD and merger rate for each model. Section 5 discusses our model assumptions and limitations, and in Section 6, we summarize and offer broader context for our results.

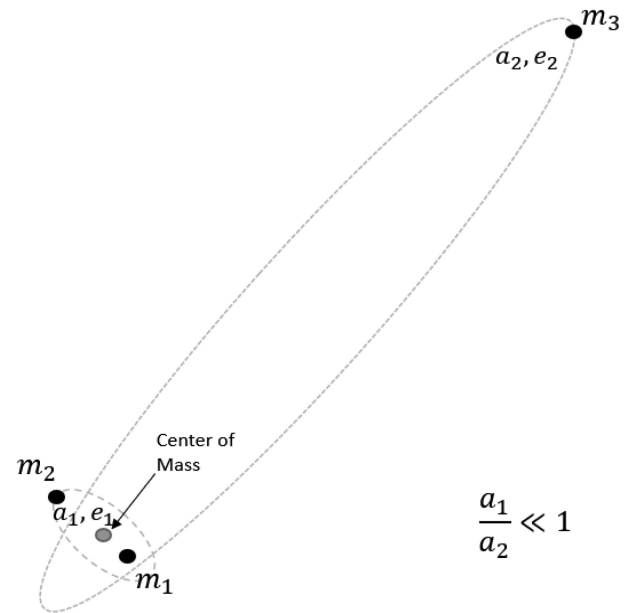


Figure 1. Illustration of a hierarchical triple system. The inner binary consists of two objects with masses m_1 and m_2 whose orbit is defined by an SMA a_1 and eccentricity e_1 . In this study, we set $e_1 = 0$. The outer binary consists of the tertiary of mass m_3 and the centre of mass of the inner binary. The orbit of the outer binary is defined by an SMA a_2 and eccentricity e_2 . The angle between the planes of the inner and outer binaries is the system inclination I .

2 BBH MERGERS FROM HIERARCHICAL TRIPLES

In the following section, we briefly describe the secular evolution of triple systems under the Lidov–Kozai resonance. For a more detailed description of this mechanism, see Naoz (2016).

2.1 Newtonian treatment

A hierarchical triple system is composed of an inner binary with masses m_1 and m_2 , and a distant tertiary of mass m_3 . The inner binary is characterized by its orbital semimajor axis (SMA) a_1 and eccentricity e_1 . The centre of mass of the inner binary then hierarchically constitutes an additional two-body system with the tertiary; this system is referred to as the outer binary, with SMA a_2 and eccentricity e_2 . Each binary defines a unique orbital plane, and the angle between these two planes is the inclination I associated with the triple system. Within these planes, the orientations of the inner and outer orbits are given by their arguments of pericentre ω_1 and ω_2 , respectively. See Fig. 1 for a diagram of a general hierarchical triple system.

A three-body system is chaotic when the system masses and separations are similar. Such a system thus tends to break apart on dynamical time-scales. Hence, on grounds of system stability, most astrophysical triple systems are hierarchical in scale, i.e. $a_1 \ll a_2$. This hierarchy of spatial scales sets a corresponding hierarchy of time-scales for these systems: the inner binary orbital period P_1 is much shorter than the outer binary orbital period P_2 , and any dynamical evolution of the system occurs on time-scales much longer than both.

When the secular approximation is applied to hierarchical triple systems, one can show that the orbital energies of each binary are

conserved quantities, and therefore the SMAs a_1 and a_2 are constant in time. Long-term changes to the system do occur, however, due to mutual torque and angular momentum transfer between the inner and outer binaries. The result of this secular evolution is simultaneous oscillations of the inner eccentricity e_1 and system inclination I , such that the total angular momentum of the triple system is conserved; at higher order, the outer orbit can evolve as well. Peak eccentricity in the inner binary occurs at the time of minimum inclination, and vice versa, and these oscillations are referred to as Lidov–Kozai cycles (Kozai 1962; Lidov 1962).

Following Miller & Hamilton (2002b) and VanLandingham et al. (2016), we define a conserved quantity derived from the quadrupole-order Hamiltonian for a hierarchical triple system:

$$W_N = -2\epsilon + \epsilon \cos^2 I + 5(1 - \epsilon) \sin^2 \omega_1 (\cos^2 I - 1), \quad (1)$$

where $\epsilon \equiv 1 - e_1^2$. The minimum value of ϵ , which corresponds to the maximum value of e_1 , occurs when $\omega_1 = \pi/2$. Hence, knowing the initial values $\omega_{1,0}$ and $e_{1,0}$, one can exploit the conservation of W to calculate the maximum value of the inner binary eccentricity, denoted e_{\max} . We note that when octupole-order effects are included, the maximal inner eccentricity reached during the evolution is usually higher than the quadrupole counterpart, and hence the BBH merger time-scale is shorter (Harrington 1968; Ford et al. 2000; Blaes et al. 2002; Thompson 2011; Naoz et al. 2013; Michaely & Perets 2014; Naoz 2016). Thus, if we were to include this effect, the fraction of BBH mergers that occur within the open cluster lifetime would be increased by a small amount. Our focus on quadrupole-level evolution is therefore conservative in the sense that we slightly underestimate this fraction.

Innanen et al. (1997) provide a concise and useful relation between the initial inclination and the maximal eccentricity due to the Lidov–Kozai resonance in the quadrupole approximation when the tertiary dominates the system angular momentum:

$$e_{\max} = \left(1 - \frac{5}{3} \cos^2 I_0\right)^{1/2}, \quad (2)$$

which implies that for the restricted three-body problem, the inner binary eccentricity tends to unity if $I_0 = \pi/2$. The growth of the inner eccentricity to its maximum value over long time-scales is a consequence of coherent perturbations by the potential of the tertiary, specifically inner binary precession. If the inner eccentricity is sufficiently high, one might expect the inner binary’s components to interact and thus to disrupt this precession. In the following subsection, we consider such an effect in general relativity (GR), namely GR pericentre precession in the inner binary.

2.2 Post-Newtonian treatment

In a triple system whose inner binary evolves to sufficiently high eccentricity, GR precession of the inner binary pericentre becomes non-negligible. This precession interferes with the coherent perturbations due to the tertiary and suppresses the Lidov–Kozai resonance. Following Miller & Hamilton (2002b), we account for this quenching effect of GR precession by adding to equation (1) the following post-Newtonian term:

$$W_{\text{PN}} = \frac{8}{\sqrt{\epsilon}} \frac{M_1}{m_3} \left(\frac{b_2}{a_1}\right)^3 \frac{GM_1}{a_1 c^2} \equiv \theta_{\text{PN}} \epsilon^{-1/2}. \quad (3)$$

Here, $M_1 \equiv m_1 + m_2$ is the total mass of the inner binary, $b_2 = a_2(1 - e_2^2)^{1/2}$ is the semiminor axis of the outer binary, G is the Newtonian gravitational constant, and c is the speed of light. Note that we include a term for GR pericentre precession but continue to

treat GW emission as negligible for the purposes of the Lidov–Kozai resonance; as a result, the sum of equations (1) and (3),

$$W = W_N + W_{\text{PN}}, \quad (4)$$

remains a conserved quantity. As before, the maximal eccentricity (minimal ϵ) is obtained when $\omega = \pi/2$, and the result in this post-Newtonian treatment becomes

$$\epsilon_{\min}^{1/2} \approx \frac{1}{6} \left(\theta_{\text{PN}} + \sqrt{\theta_{\text{PN}}^2 + 60 \cos^2 I_0}\right). \quad (5)$$

This maximal eccentricity can be used to estimate the merger time of the inner binary due to GW emission. The merger time-scale for a binary of eccentricity $e \approx 1$ is given by Peters (1964) as

$$T_{\text{GW}} \approx \frac{768}{425} T_c(a_1)(1 - e^2)^{7/2}, \quad (6)$$

where $T_c \equiv a_1^4/\beta$ is the merger time-scale for a circular binary and $\beta \equiv 64G^3 m_1 m_2 (m_1 + m_2)/(5c^5)$. However, in the case of a triple system whose inner binary oscillates between its initial eccentricity $e_{1,0}$ and maximal eccentricity e_{\max} , the merger time-scale due to GW emission is necessarily longer. Randall & Xianyu (2018) analytically estimate the merger time in this case to be

$$T_{\text{merger}} = \frac{T_{\text{GW}}}{\epsilon_{\min}^{1/2}}. \quad (7)$$

In this work, we are interested in merger times $T_{\text{merger}} < T_{\text{Hubble}}$ for the purpose of calculating the merger rate density and DTD of BBH mergers originating from hierarchical triples. In the following section, we describe a method for numerically selecting different triple populations in order to calculate these statistics.

3 NUMERICAL METHOD

Our approach to calculating merger rate densities and DTDs is as follows. In each of several population models, described in Sections 3.2 and 3.3, we employ a Monte Carlo simulation to generate 10^6 representative triple systems. For each triple system in a given model, the model analytically determines whether an inner BBH merger occurs within T_{Hubble} using equation (7) and records the value of T_{merger} in order to calculate the theoretical DTD.

As stated earlier, we assume that star formation occurs entirely within open clusters (Lada & Lada 2003) and that as a result, BH progenitor stars all form simultaneously, i.e. we do not calculate any detailed dynamical effects during the main-sequence (MS) phase.

Note that we ignore secular evolution during the short MS phase. If a triple system undergoes substantial eccentricity oscillations during the MS phase, then the inner binary stars, prior to their evolution into compact objects, will essentially decouple their dynamical evolution from the triple system (e.g. Naoz 2016; Hamers & Thompson 2019). This happens because tidal interactions introduce an additional precession term which quenches the Lidov–Kozai oscillation. In this case, the evolution of the massive stars is similar to classical isolated binary evolution, which is the first channel described in the introduction (e.g. Tutukov & Yungelson 1973, 1993; Lipunov et al. 1997; Bethe & Brown 1998; Portegies Zwart & Yungelson 1998; Kalogera 2000; Voss & Tauris 2003; Kalogera et al. 2007; Belczynski et al. 2008, 2016; Mandel & O’Shaughnessy 2010; Dominik et al. 2012, 2013, 2015; de Mink & Belczynski 2015; Eldridge et al. 2017; Giacobbo et al. 2018; Olejak et al. 2020).

3.1 Creating a population model

Each population model uses a Monte Carlo approach to generate a set of stable, hierarchical triple systems whose inner binaries evolve to BBHs. Although binary stellar evolution processes are beyond the scope of this study, we do consider basic restrictions imposed on triple systems due to their passage through the MS phase. Specifically, in some models we exclude triples whose inner binary components would have interacted as MS stars. We exclude any triple that is considered dynamically unstable by the criterion of Mardling & Aarseth (2001). Additionally, we work under the simplifying assumption that the probability distributions of all system parameters are independent, meaning that an individual triple system can be generated by drawing each of its parameters independently.

Triple systems are produced in this model by drawing initial stellar masses and orbital parameters, then mapping those stellar masses to final BH masses. To generate the inner binary for a system, we draw the primary mass m_1 from the Kroupa initial mass function (IMF; Kroupa 2001), denoted $f_{\text{IMF}}(m)$, with a range $[m_{\text{min}}, m_{\text{max}}]$. Because we are interested in masses of BH progenitors, we concern ourselves only with the upper end of the range of initial masses. The Kroupa and Salpeter IMFs (Salpeter 1955) are similar in the high-mass regime, and therefore we do not expect that a different choice of IMF would affect the results presented here. However, the specific choice of IMF is important for the normalization of the results (see Section 4.1).

With m_1 determined, the next parameter drawn is the inner binary SMA, a_1 . Motivated by observations (Duchêne & Kraus 2013; Moe & Di Stefano 2017), we draw the inner SMA from a log-uniform distribution (Öpik’s law) over a range $[a_{1,\text{min}}, a_{1,\text{max}}]$. The mass of the second inner binary object is determined by

$$m_2 = m_1 q_1, \quad (8)$$

where q_1 is the inner binary mass ratio, drawn from a power-law distribution $f(q) \propto q^\gamma$. For high-mass stars ($M_* \gtrsim 16 M_\odot$), this distribution covers the range $[0.1, 1]$. The power-law index γ is determined by the SMA of the inner binary, with $\gamma = 0$ for $a_1 < 100$ au and $\gamma = -1/2$ for $a_1 > 100$ au (Duchêne & Kraus 2013).

The remaining parameters of the inner binary orbit are its eccentricity e_1 and argument of pericentre ω_1 . In order to be conservative in our calculation of merger times, we set the inner binary eccentricity to be zero, $e_1 \rightarrow 0$. Any other choice of inner eccentricity distribution would shorten the merger time-scale by increasing the maximal eccentricity reached in the Lidov–Kozai resonance (Lidov & Ziglin 1976; Naoz 2016). Finally, ω_1 is drawn from a uniform distribution on $[0, 2\pi]$. These five parameters define our inner binary progenitor star system.

As mentioned previously, we discard any system whose inner binary would have interacted during the MS phase. To check for such interactions, our method calculates the radii of the progenitor stars and compares these to the stars’ respective Roche limits. The stellar radius–mass relation is given by $r_i \propto m_i^{0.57}$ (Demircan & Kahraman 1991) and the Roche limit by

$$R_{1(2)} = a_1 \times \frac{0.49 q_{1(2)}^{2/3}}{0.6 q_{1(2)}^{2/3} + \ln(1 + q_{1(2)}^{1/3})}, \quad (9)$$

where $q_{1(2)} = m_{1(2)}/m_{2(1)}$ (Eggleton 1983). A system is discarded if $r_i > R_i$ for either progenitor star, reflecting the likelihood that such a system would have interacted significantly during the MS phase and might have failed to produce a BBH.

We now address the parameters characterizing the outer binary. The tertiary mass m_3 is set by drawing the outer mass ratio $q_2 \equiv$

m_3/M_1 from a power-law distribution $q \propto M_1^\gamma$ with $\gamma = -2$ (Moe & Di Stefano 2017) over a range $[0.1, 1]$. The outer eccentricity e_2 is drawn from a thermal distribution $f(e) = 2e$ and the outer SMA a_2 from a log-uniform distribution over a range $[a_{2,\text{min}}, a_{2,\text{max}}]$. The final parameter needed to specify the triple system is the mutual orbital inclination I ; this value is drawn from a distribution function $f(I)$ which varies by model and is discussed further in the following sections.

With the system parameters fully determined, our method next checks that the triple is indeed dynamically stable. The outer pericentre distance is given by $R_p^{\text{out}} = a_2(1 - e_2)$, and Mardling & Aarseth (2001) define the stability threshold

$$\kappa = 2.8 \left[(1 + q_2) \frac{(1 + e_2)}{(1 - e_2)} \right]^{2/5} a_1, \quad (10)$$

which specifies the smallest outer pericentre value for which the system remains stable. Accordingly, a system is discarded by our model if $R_p^{\text{out}} < \kappa$.

The steps described to this point are sufficient to generate a stable, hierarchical, stellar triple. The initial masses of the three system components must now be mapped to the final masses of the BHs or other objects to which they evolve. When the simulation generates a star of sufficient mass, it converts it into a BH by establishing two mass regimes. For a star whose initial mass m_i falls in the range $20 M_\odot \leq m_i \leq 60 M_\odot$, the resulting BH is assigned a final mass $m_i/2$, in keeping with the approximate relation between progenitor mass and final BH mass for stars in this range. A star with initial mass $m_i > 60 M_\odot$ is converted to a BH with a final mass of $30 M_\odot$, reflecting the significant mass-loss experienced by very massive MS stars.

The tertiary is treated differently from the initial binary, as it does not necessarily evolve to a BH. For $m_3 \leq 8 M_\odot$, the simulation checks the MS lifetime for that mass; if it is less than T_{merger} , then m_3 is converted to a $1 M_\odot$ white dwarf. In this case, we ignore any expansion of the outer SMA a_2 , given that the expected mass-loss of the tertiary stellar companion in this case is negligible relative to the total mass of the triple. To obtain the total merger time, the original MS lifetime is then added to the merger time for the white dwarf system.

For a tertiary in the range $8 M_\odot < m_3 < 20 M_\odot$, i.e. the mass range for forming a neutron star (NS), the calculation is stopped and the system discarded. In this case, it is expected that the triple system will be disrupted by the natal kick of the NS (Hobbs et al. 2005), precluding any secular evolution.

The following section introduces the baseline (‘standard’) population model, which adopts the most plausible assumptions for the various triple system parameter distributions. A set of additional models then extends the standard model by modifying a single assumption at a time.

3.2 Standard model

The baseline model assumes that BHs are formed with no natal kicks, because of either a failed supernova or massive fallback. The limits on the primary mass are set to $m_{1,\text{min}} = 30 M_\odot$ and $m_{1,\text{max}} = 100 M_\odot$. While $20 M_\odot$ O-type stars might produce BHs, there is considerable speculation regarding which mass ranges will yield a natal kick when forming compact objects. By raising the minimum mass for BH formation in our simulation, we impose a conservative buffer which makes it more likely that natal kicks can be neglected.

This model sets the bounds on the inner binary SMA to $a_{1,\text{min}} = 0.1$ au and $a_{1,\text{max}} = 100$ au. In keeping with the focus on hierarchical triples, the outer binary SMA is assigned a lower bound of $a_{2,\text{min}} = 5a_1$ and an upper bound of $a_{2,\text{max}} = 1000$ au. This upper

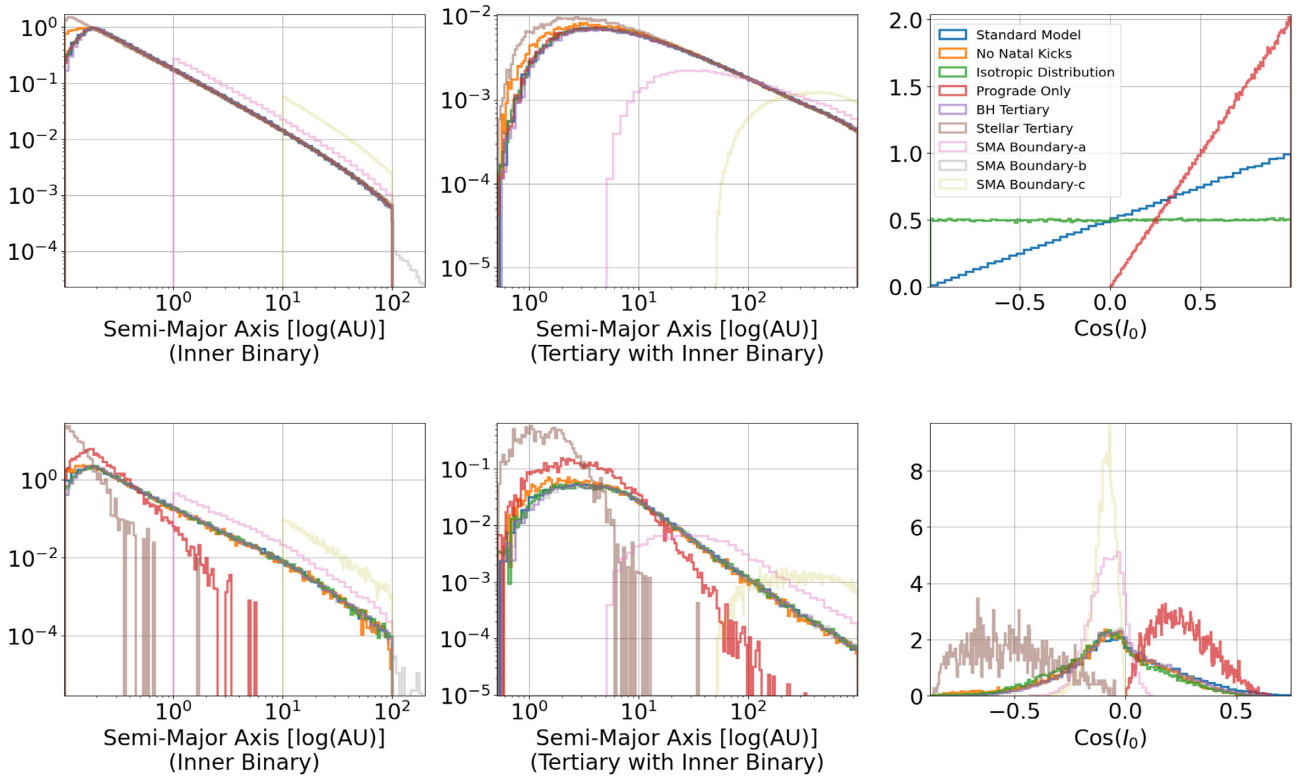


Figure 2. Top row: Initial parameter distributions produced by the Monte Carlo simulation for the various population models. Left-hand panel: inner binary SMA; middle panel: outer binary SMA; right-hand panel: system inclination plotted as $\cos i_0$. Note that in the distribution of inclinations, only the standard, isotropic, and prograde models are shown; all others exhibit no significant differences from the standard model in their distributions of inclinations. Bottom row: the same three parameter distributions shown in the top row, but restricted to the subset of triple systems which merge within a Hubble time in our model. All plots are normalized to unity.

bound is determined by the environment: we do not expect open clusters to contain ultra-wide systems, as these would be ionized due to the relatively high stellar density in the cluster. For a more detailed treatment of the open cluster environment, see Section 5. As mentioned in Section 3.1, the distributions of both the inner SMA, a_1 , and outer SMA, a_2 are log-uniform.

The inclination I of each system is of particular interest when studying the Lidov–Kozai resonance. Given the dearth of observational constraints on the inclinations of high-multiplicity systems within open clusters, we make the reasonable assumption that open clusters and their constituents exhibit a bias towards aligned angular momenta. For triple systems, such a bias favours coplanar orbits. To account for this preference, the standard model draws inclinations from a distribution that increases linearly with $\cos I$ in the range $\cos I \in [-1, 1]$ (see Fig. 2).

3.3 Additional models

To probe the sensitivity of merger rates and the DTD to the assumptions used in the standard model, we present several additional models. Each isolates and modifies a single assumption in order to test the robustness of our results.

3.3.1 No natal kicks

The standard model excludes primary object masses below $m_{1,\min} = 30 M_\odot$ due to uncertainty regarding BH natal kicks below this mass. In this no natal kicks model, it is assumed that *all* BHs are born with

no natal kick, and thus $m_{1,\min}$ is lowered to the traditionally accepted lower limit of $20 M_\odot$ for BH progenitors.

3.3.2 Isotropic distribution

In order to test the sensitivity of our results to the initial distribution of mutual inclinations, this model implements an isotropic (rather than prograde-biased) distribution for I . Inclinations are drawn from a uniform distribution of $\cos I \in [-1, 1]$, i.e. from prograde to retrograde mutual inclinations. See Fig. 2 for the distribution of inclinations generated by this model.

3.3.3 Prograde-only

This model restricts the mutual inclination I to prograde values by drawing from a linear distribution of $\cos I \in [0, 1]$. See again Fig. 2 for the initial distribution of inclinations.

3.3.4 BH tertiary

This and the following model concern modifications to the tertiary object in the triple system. In the standard model, the tertiary star is either massive enough to become a BH, forming a hierarchical triple BH, or has a mass low enough to evolve to a white dwarf. Recall that if the tertiary mass falls in the intermediate regime $8 M_\odot < m_3 < 20 M_\odot$, it is assumed to form a NS and disrupt the triple via a high natal kick velocity. In this BH tertiary population model, only tertiary

companions which form BHs are included, and so only systems with tertiary masses $m_3 > 20 M_\odot$ are considered.

3.3.5 Stellar tertiary

Complementary to the previous model, here only lower-mass tertiary objects are allowed. The evolution of these stars is modelled in two phases, as previously described in Section 3.1. In the first, a star retains its zero-age MS mass m_3 . In the second phase, the mass of the tertiary star is set to $1 M_\odot$ to account for mass-loss during the giant phases and final evolution to a white dwarf. As before, these low-mass tertiaries are restricted to $m_3 \leq 8 M_\odot$.

3.3.6 SMA boundaries model a

In all previous models, the inner binary SMA a_1 is drawn from the range [0.1 au, 100 au]. This model considers only larger inner binaries by increasing the lower bound of the inner binary SMA by an order of magnitude, drawing $a_1 \in [1 \text{ au}, 100 \text{ au}]$.

3.3.7 SMA boundaries model b

This model complements the previous model by doubling the upper bound on the inner binary SMA, drawing $a_1 \in [0.1 \text{ au}, 200 \text{ au}]$.

3.3.8 SMA boundaries model c

To fully rule out any possible interaction of the inner binary components while they are in the MS phase, this model draws the inner binary SMA from the range, $a_1 \in [10 \text{ au}, 100 \text{ au}]$. In this case, the inner binary components will not overflow their mutual Roche sphere during their binary stellar evolution (Antonini et al. 2017).

4 RESULTS

4.1 Normalization and rates

We calculate the merger rate density for Lidov–Kozai-assisted BBHs under the assumption that the Milky Way is the prototypical spiral galaxy with a population of $N \approx 10^{10}$ stars. The fraction of primary objects in our triple systems that will form BHs is given by

$$f_p = \frac{\int_{30 M_\odot}^{100 M_\odot} m^{-2.3} dm}{\int_{0.08 M_\odot}^{100 M_\odot} f_{\text{IMF}}(m) dm}. \quad (11)$$

We continue to treat BHs as forming in high-multiplicity systems (Duchêne & Kraus 2013) and without natal kicks. Therefore, taking a uniform distribution of mass ratios $q_1 \in [0.1, 1]$ for the inner binary, the fraction of secondary stars forming BHs is $f_s \approx 0.4$. Drawing from a mass ratio distribution $q_2 \propto M_1^{-2}$ for a tertiary at large distances to the inner binary, the fraction of tertiary objects that remain in triple systems is $f_t \approx 0.25$. Recall that all tertiary masses in the range $[8 M_\odot, 30 M_\odot]$ are rejected, as these are expected to disrupt the triple system due to large natal kicks during NS formation (Hobbs et al. 2005). The fraction of the total stellar population which resides in triple systems is taken to be $f_{\text{triple}} \approx 0.1$ (Tokovinin 2004). Recall that because this work concerns triples within open clusters, we consider only those triples with a maximum outer binary SMA of 1000 au and maximum inner binary SMA of 100 au; see Section 5 for a discussion of this choice of values. The fraction of stars which form

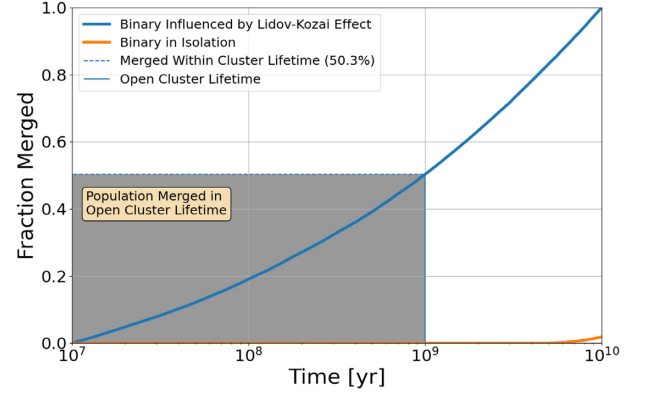


Figure 3. DTD for simulated mergers in the standard model. The blue curve shows the distribution function for systems which merged within a Hubble time. The grey box indicates the fraction of mergers occurring during the open cluster phase, using 10^9 yr as the upper limit of an open cluster lifetime. For comparison, the orange curve shows the DTD that would result if all BBHs merged in isolation via GW emission alone.

triple systems with inner binary BBHs that merge via the Lidov–Kozai resonance is then given by

$$F_{\text{model}} = 10^{-5} \left(\frac{f_p}{10^{-3}} \right) \left(\frac{f_s}{0.4} \right) \left(\frac{f_t}{0.25} \right) \left(\frac{f_{\text{triple}}}{0.1} \right) f_{\text{merger}}, \quad (12)$$

where f_{merger} is the merger fraction for hierarchical triples calculated by our numerical model. Recall that a triple system is considered to have merged if $T_{\text{merger}} < T_{\text{Hubble}}$. The average merger rate for a single Milky Way-like galaxy over a Hubble time is therefore

$$\Gamma_{\text{MW}} = N \times \frac{F_{\text{model}}}{T_{\text{Hubble}}} \approx 0.53 \text{ Myr}^{-1}. \quad (13)$$

Following Belczynski et al. (2016), the merger rate density in the local Universe is given by

$$\mathcal{R} = \rho_{\text{gal}} \times N \times \frac{F_{\text{model}}}{T_{\text{Hubble}}} \approx 6 \left(\frac{F_{\text{model}}}{10^{-5}} \right) \text{ Gpc}^{-3} \text{ yr}^{-1}, \quad (14)$$

where $\rho_{\text{gal}} \approx 0.0116 \text{ Mpc}^{-3}$ is the Milky Way-like galaxy density in the local Universe (Belczynski et al. 2016). Depending on the values of the factors that determine F_{model} (see equation 12 above), this rate is plausibly comparable to the observed LIGO rate of $\sim 20 \text{ Gpc}^{-3} \text{ yr}^{-1}$.

4.2 Delay-time distribution

Having recorded T_{merger} for each triple system, we can calculate the fraction of systems which merge within a given time after star formation. Fig. 3 shows the standard model DTD, i.e. the cumulative merger fraction as a function of time. We find that approximately half of mergers in the standard model occur within the lifetime of open clusters, suggesting that a significant fraction of Lidov–Kozai-induced mergers may occur in these clusters before their dissolution.

Fig. 4 compares the DTD for the standard model to those for the additional models. Accounting for white dwarf formation in low-mass tertiaries and allowing all viable systems to evolve in time, we find that ~ 20 – 50 per cent of Lidov–Kozai-assisted BBH mergers occur within the lifetime of open clusters. We find that the DTD is not particularly sensitive to model assumptions, with the exception of the stellar tertiary model, which is skewed towards later merger times and yields a smaller merger fraction within the lifetime of open clusters. This difference can be understood as the result of lower-mass

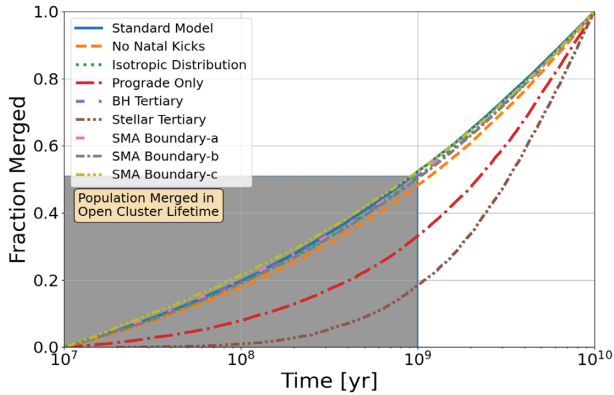


Figure 4. Comparison of DTDs for simulated mergers across all population models. Curves show the distribution function for systems that merged within a Hubble time in all models. The grey box indicates the fraction of mergers that occurred during the open cluster phase in the standard model. The distribution shows little sensitivity to initial assumptions, with the exception of low tertiary masses in the stellar tertiary model.

tertiary objects, which have weaker effects on the secular evolution of triple systems.

5 DISCUSSION

5.1 Assumptions

Each of the population models developed in this work rests on a set of underlying assumptions regarding the parameter distributions of its triple systems. In what follows, we discuss the justification for and implications of several key model assumptions.

5.1.1 BH natal kicks

The first and most important of these assumptions is that BHs are born with little or no natal kick. While it remains unclear whether such kicks are significant (Nelemans, Tauris & van den Heuvel 1999; Willems et al. 2005; Repetto, Davies & Sigurdsson 2012; Wong et al. 2012, 2014; Mandel 2016; Repetto, Igoshev & Nelemans 2017), observational evidence supports BH formation via failed supernova or direct collapse (Fryer, Woosley & Hartmann 1999; Ertl et al. 2016; Adams et al. 2017). Both mechanisms imply small natal kicks or none at all, supporting the use of our simplifying assumption. In future work, however, we aim to test the importance and sensitivity of this assumption by implementing a more sophisticated population synthesis method.

5.1.2 Triple formation

Throughout this study, we assume that all star formation occurs in open clusters or associations (Lada & Lada 2003). The issue of triple formation is not explicitly addressed; our standard model effectively treats each hierarchical triple as primordial. This assumption of primordial system formation is reflected in the non-isotropic distribution of inclinations used in the standard model. We explore a deviation from this assumption by including the isotropic distribution model, which draws from a uniform distribution of $\cos I$ and thus simulates triples formed by dynamical processes. In our results, neither the merger rate density nor the DTD depends sensitively on the initial distribution of inclinations.

5.1.3 SMA bounds

In the standard model, the lower bound on the inner binary SMA is set to $a_{1,\min} = 0.1$ au. For an isolated BBH with $m_1 = m_2 = 20 M_\odot$ and $a_1 = 0.1$ au in a circular orbit, equation (6) gives an inspiral time (via GW emission only) of $T_{\text{GW}} \approx 10^{10}$ yr, which is of the order of a Hubble time. Therefore, for smaller values of $a_{1,\min}$, we would not expect our Lidov–Kozai channel to increase the overall rate of BBH mergers. The upper bound $a_{2,\max}$ on the outer binary SMA is set by environmental constraints, specifically the lifetime of a wide orbit in a collisional environment. Following Bahcall, Hut & Tremaine (1985), one can calculate the half-life of a wide system of SMA a_2 in a collisional environment according to

$$t_{1/2} = 0.00233 \frac{v_{\text{enc}}}{G m_p n_* a_2}, \quad (15)$$

where v_{enc} is the typical encounter velocity at infinity, m_p is the mass of the perturbing body, and n_* is the local stellar number density. For an open cluster, we take v_{enc} to be a typical velocity dispersion $\sigma \approx 5 \text{ km s}^{-1}$, and assume a stellar number density $n_* \approx 0.5 \text{ pc}^{-3}$ and a perturber mass $m_p = 1 M_\odot$. Taking 10^9 yr to be a typical open cluster lifetime, the outer binary SMA of a system whose half-life is equal to the lifetime of the cluster is $a_2 \approx 1000$ au; this serves as the upper limit for the size of the outer binary.

5.2 Mergers in the open cluster phase

As summarized in Fig. 4 and in Table 1 for all models considered, the fraction of mergers occurring during the lifetime of open clusters is significant. In the standard model, assuming an open cluster lifetime of 10^9 Myr (10^8 Myr), we find that 49.9 per cent (18.9 per cent) of BBH mergers induced by the Lidov–Kozai resonance occur in open clusters. This result implies that at least this fraction of mergers from the secular triple channel occur in young environments within star-forming galaxies.

6 CONCLUSIONS

In this work, we calculate the merger rates and DTD of BBH mergers occurring in hierarchical triple systems within open clusters via the Lidov–Kozai resonance. This resonance increases the inner binary eccentricity in cycles, allowing the binary to dissipate orbital energy and inspiral via GW emission. Given the sensitive dependence of merger time on orbital eccentricity, BBH mergers in triple systems experiencing the Lidov–Kozai resonance are expected to occur on much shorter time-scales than those in isolated binaries. Calculating the DTD for hierarchical triples in open clusters, we find that a significant fraction of mergers (18–50 per cent in our baseline model) occur before the open cluster has dissolved. This result suggests that many mergers in hierarchical triples occur in star-forming regions and hence in spiral galaxies.

ACKNOWLEDGEMENTS

EM thanks the University of Maryland CTC prize fellowship for supporting this research. The authors thank Selma de Mink, Chris Belczynski, and Ilya Mandel for their useful comments on this manuscript.

DATA AVAILABILITY

The data underlying this article will be shared on reasonable request to the corresponding author.

Table 1. Parameter distributions and merger results for the standard and additional models. For comparison with the lifetimes of open clusters, the percentages of systems that have merged at 10^8 and 10^9 yr are reported.

Model	m_1 (M_\odot)	m_3 (M_\odot)	Inclination [$f(I)$]	a_1 (au)	Local rate ($\text{Gpc}^{-3} \text{yr}^{-1}$)	Merger time $\leq 10^9$ yr (10^8 yr) (per cent)
Standard	30–100	$m \leq 8$ $m \geq 30$	Linear in $\cos I$	0.1–100	6.2	49.9 (18.9)
No natal kicks	20–100	$m \leq 8$ $m \geq 20$	Linear in $\cos I$	0.1–100	4.5	48.4 (18.1)
Isotropic distribution	30–100	$m \leq 8$ $m \geq 30$	Uniform in $\cos I$	0.1–100	6.6	51.0 (19.5)
Prograde-only	30–100	$m \leq 8$ $m \geq 30$	Linear in $\cos I$, $0 \leq I \leq 1$	0.1–100	2.1	33.3 (7.9)
BH tertiary	30–100	$m \geq 30$	Linear in $\cos I$	0.1–100	6.7	50.5 (19.3)
Stellar tertiary	30–100	$m \leq 8$	Linear in $\cos I$	0.1–100	0.9	15.8 (0.6)
SMA boundaries a	30–100	$m \leq 8$ $m \geq 30$	Linear in $\cos I$	1–100	3.7	51.5 (20.0)
SMA boundaries b	30–100	$m \leq 8$ $m \geq 30$	Linear in $\cos I$	0.1–200	6.2	33.3 (7.9)
SMA boundaries c	30–100	$m \leq 8$ $m \geq 30$	Linear in $\cos I$	10–100	2.1	51.2 (21)

REFERENCES

- Abbott R. et al., 2020, preprint ([arXiv:2010.14527](https://arxiv.org/abs/2010.14527))
- Adams S. M., Kochanek C. S., Gerke J. R., Stanek K. Z., Dai X., 2017, *MNRAS*, 468, 4968
- Antonini F., Perets H. B., 2012, *ApJ*, 757, 27
- Antonini F., Murray N., Mikkola S., 2014, *ApJ*, 781, 45
- Antonini F., Chatterjee S., Rodriguez C. L., Morscher M., Pattabiraman B., Kalogera V., Rasio F. A., 2016, *ApJ*, 816, 65
- Antonini F., Toonen S., Hamers A. S., 2017, *ApJ*, 841, 77
- Bahcall J. N., Hut P., Tremaine S., 1985, *ApJ*, 290, 15
- Banerjee S., 2018, *MNRAS*, 473, 909
- Belczynski K., Kalogera V., Rasio F. A., Taam R. E., Zezas A., Bulik T., Maccarone T. J., Ivanova N., 2008, *ApJS*, 174, 223
- Belczynski K., Repetto S., Holz D. E., O’Shaughnessy R., Bulik T., Berti E., Fryer C., Dominik M., 2016, *ApJ*, 819, 108
- Bethe H. A., Brown G. E., 1998, *ApJ*, 506, 780
- Blaes O., Lee M. H., Socrates A., 2002, *ApJ*, 578, 775
- de Mink S. E., Belczynski K., 2015, *ApJ*, 814, 58
- de Mink S. E., Mandel I., 2016, *MNRAS*, 460, 3545
- Demircan O., Kahraman G., 1991, *Ap&SS*, 181, 313
- Di Carlo U. N., Giacobbo N., Mapelli M., Pasquato M., Spera M., Wang L., Haardt F., 2019, *MNRAS*, 487, 2947
- Di Carlo U. N. et al., 2020, *MNRAS*, 498, 495
- Dominik M., Belczynski K., Fryer C., Holz D. E., Berti E., Bulik T., Mandel I., O’Shaughnessy R., 2012, *ApJ*, 759, 52
- Dominik M., Belczynski K., Fryer C., Holz D. E., Berti E., Bulik T., Mandel I., O’Shaughnessy R., 2013, *ApJ*, 779, 72
- Dominik M. et al., 2015, *ApJ*, 806, 263
- Duchêne G., Kraus A., 2013, *ARA&A*, 51, 269
- Eggleton P. P., 1983, *ApJ*, 268, 368
- Eldridge J. J., Stanway E. R., Xiao L., McClelland L. A. S., Taylor G., Ng M., Greis S. M. L., Bray J. C., 2017, *Publ. Astron. Soc. Aust.*, 34, e058
- Ertl T., Janka H. T., Woosley S. E., Sukhbold T., Ugliano M., 2016, *ApJ*, 818, 124
- Ford E. B., Kozinsky B., Rasio F. A., 2000, *ApJ*, 535, 385
- Fragione G., Kocsis B., 2018, *Phys. Rev. Lett.*, 121, 161103
- Fragione G., Grishin E., Leigh N. W. C., Perets H. B., Perna R., 2019, *MNRAS*, 488, 47
- Fryer C. L., Woosley S. E., Hartmann D. H., 1999, *ApJ*, 526, 152
- Giacobbo N., Mapelli M., Spera M., 2018, *MNRAS*, 474, 2959
- González E., Kremer K., Chatterjee S., Fragione G., Rodríguez C. L., Weatherford N. C., Ye C. S., Rasio F. A., 2021, *ApJ*, 908, L29
- Gültekin K., Miller M. C., Hamilton D. P., 2004, *ApJ*, 616, 221
- Gültekin K., Miller M. C., Hamilton D. P., 2006, *ApJ*, 640, 156
- Hamers A. S., Thompson T. A., 2019, *ApJ*, 883, 23
- Hamers A. S., Bar-Or B., Petrovich C., Antonini F., 2018, *ApJ*, 865, 2
- Hamilton C., Rafikov R. R., 2019, *MNRAS*, 488, 5512
- Harrington R. S., 1968, *AJ*, 73, 190
- Hoang B.-M., Naoz S., Kocsis B., Rasio F. A., Dosopoulou F., 2018, *ApJ*, 856, 140
- Hobbs G., Lorimer D. R., Lyne A. G., Kramer M., 2005, *MNRAS*, 360, 974
- Innanen K. A., Zheng J. Q., Mikkola S., Valtonen M. J., 1997, *AJ*, 113, 1915
- Kalogera V., 2000, *ApJ*, 541, 319
- Kalogera V., Belczynski K., Kim C., O’Shaughnessy R., Willems B., 2007, *Phys. Rep.*, 442, 75
- Kimpson T. O., Spera M., Mapelli M., Ziosi B. M., 2016, *MNRAS*, 463, 2443
- Kozai Y., 1962, *AJ*, 67, 591
- Kroupa P., 2001, *MNRAS*, 322, 231
- Kulkarni S. R., Hut P., McMillan S., 1993, *Nature*, 364, 421
- Kumamoto J., Fujii M. S., Tanikawa A., 2019, *MNRAS*, 486, 3942
- Lada C. J., Lada E. A., 2003, *ARA&A*, 41, 57
- Leigh N. W. C. et al., 2018, *MNRAS*, 474, 5672
- Lidov M. L., 1962, *Planet. Space Sci.*, 9, 719
- Lidov M. L., Ziegler S. L., 1976, *Celest. Mech.*, 13, 471
- Lipunov V. M., Postnov K. A., Prokhorov M. E., 1997, *MNRAS*, 288, 245
- Liu B., Lai D., 2018, *ApJ*, 863, 68
- Madau P., Rees M. J., 2001, *ApJ*, 551, L27
- Mandel I., 2016, *MNRAS*, 456, 578
- Mandel I., de Mink S. E., 2016, *MNRAS*, 458, 2634
- Mandel I., O’Shaughnessy R., 2010, *Class. Quantum Gravity*, 27, 114007
- Marchant P., Langer N., Podsiadlowski P., Tauris T. M., Moriya T. J., 2016, *A&A*, 588, A50
- Mardling R. A., Aarseth S. J., 2001, *MNRAS*, 321, 398
- Martinez M. A. S. et al., 2020, *ApJ*, 903, 67

- McKernan B., Ford K. E. S., Lyra W., Perets H. B., 2012, *MNRAS*, 425, 460
- Michaely E., 2021, *MNRAS*, 500, 5543
- Michaely E., Perets H. B., 2014, *ApJ*, 794, 122
- Michaely E., Perets H. B., 2018, *ApJ*, 855, L12
- Michaely E., Perets H. B., 2019, *ApJ*, 887, L36
- Michaely E., Perets H. B., 2020, *MNRAS*, 498, 4924
- Miller M. C., Hamilton D. P., 2002a, *MNRAS*, 330, 232
- Miller M. C., Hamilton D. P., 2002b, *ApJ*, 576, 894
- Miller M. C., Lauburg V. M., 2009, *ApJ*, 692, 917
- Moe M., Di Stefano R., 2017, *ApJS*, 230, 15
- Moraux E., 2016, in Moraux E., Lebreton Y., Charbonnel C., eds, *EAS Publ. Ser. Vol. 80, Stellar Clusters: Benchmarks of Stellar Physics and Galactic Evolution - EES2015. Les Ulis: EDP Sciences*, p. 73
- Naoz S., 2016, *ARA&A*, 54, 441
- Naoz S., Farr W. M., Lithwick Y., Rasio F. A., Teysandier J., 2013, *MNRAS*, 431, 2155
- Nelemans G., Tauris T. M., van den Heuvel E. P. J., 1999, *A&A*, 352, L87
- Olejak A., Fishbach M., Belczynski K., Holz D. E., Lasota J. P., Miller M. C., Bulik T., 2020, *ApJ*, 901, L39
- Peters P. C., 1964, *Phys. Rev.*, 136, 1224
- Petrovich C., Antonini F., 2017, *ApJ*, 846, 146
- Portegies Zwart S. F., McMillan S. L. W., 2000, *ApJ*, 528, L17
- Portegies Zwart S. F., Yungelson L. R., 1998, *A&A*, 332, 173
- Randall L., Xianyu Z.-Z., 2018, *ApJ*, 864, 134
- Repetto S., Davies M. B., Sigurdsson S., 2012, *MNRAS*, 425, 2799
- Repetto S., Igoshev A. P., Nelemans G., 2017, *MNRAS*, 467, 298
- Rodriguez C. L., Chatterjee S., Rasio F. A., 2016, *Phys. Rev. D*, 93, 084029
- Rodriguez C. L., Amaro-Seoane P., Chatterjee S., Kremer K., Rasio F. A., Samsing J., Ye C. S., Zevin M., 2018, *Phys. Rev. D*, 98, 123005
- Rodriguez C. L., Kremer K., Chatterjee S., Fragione G., Loeb A., Rasio F. A., Weatherford N. C., Ye C. S., 2021, *Res. Notes Am. Astron. Soc.*, 5, 19
- Salpeter E. E., 1955, *ApJ*, 121, 161
- Samsing J., D’Orazio D. J., 2018, *MNRAS*, 481, 5445
- Samsing J., MacLeod M., Ramirez-Ruiz E., 2014, *ApJ*, 784, 71
- Sigurdsson S., Phinney E. S., 1993, *ApJ*, 415, 631
- Silber K., Tremaine S., 2017, *ApJ*, 836, 39
- Stone N. C., Metzger B. D., Haiman Z., 2017, *MNRAS*, 464, 946
- Thompson T. A., 2011, *ApJ*, 741, 82
- Tokovinin A., 2004, in Allen C., Scarfe C., eds, *Rev. Mex. Astron. Astrofis. Conf. Ser. Vol. 27, Environment and Evolution of Double and Multiple Stars*. p. 7
- Tutukov A., Yungelson L., 1973, *Nauchnye Informatsii*, 27, 70
- Tutukov A. V., Yungelson L. R., 1993, *MNRAS*, 260, 675
- VanLandingham J. H., Miller M. C., Hamilton D. P., Richardson D. C., 2016, *ApJ*, 828, 77
- Vigna-Gómez A., Toonen S., Ramirez-Ruiz E., Leigh N. W. C., Riley J., Haster C.-J., 2021, *ApJ*, 907, L19
- Voss R., Tauris T. M., 2003, *MNRAS*, 342, 1169
- Wang H., Stephan A. P., Naoz S., Hoang B.-M., Breivik K., 2020, preprint ([arXiv:2010.15841](https://arxiv.org/abs/2010.15841))
- Weatherford N. C., Fragione G., Kremer K., Chatterjee S., Ye C. S., Rodriguez C. L., Rasio F. A., 2021, *ApJ*, 907, L25
- Willems B., Henninger M., Levin T., Ivanova N., Kalogera V., McGhee K., Timmes F. X., Fryer C. L., 2005, *ApJ*, 625, 324
- Wong T.-W., Valsecchi F., Fragos T., Kalogera V., 2012, *ApJ*, 747, 111
- Wong T.-W., Valsecchi F., Ansari A., Fragos T., Glebbeek E., Kalogera V., McClintock J., 2014, *ApJ*, 790, 119

This paper has been typeset from a $\text{\TeX}/\text{\LaTeX}$ file prepared by the author.